

Lawrence Berkeley National Laboratory

LBL Publications

Title

Transmission in situ and operando high temperature X-ray powder diffraction in variable gaseous environments

Permalink

<https://escholarship.org/uc/item/59j8g7x9>

Journal

Review of Scientific Instruments, 89(3)

ISSN

0034-6748

Authors

Schlicker, Lukas

Doran, Andrew

Schneppmüller, Peter

et al.

Publication Date

2018-03-01

DOI

10.1063/1.5001695

Peer reviewed

Transmission in situ and operando high temperature X-ray powder diffraction in variable gaseous environments

Lukas Schlicker, Andrew Doran, Peter Schnepfmüller, Albert Gili, Mathias Czasny, Simon Penner, and Aleksander Gurlo

Citation: [Review of Scientific Instruments](#) **89**, 033904 (2018); doi: 10.1063/1.5001695

View online: <https://doi.org/10.1063/1.5001695>

View Table of Contents: <http://aip.scitation.org/toc/rsi/89/3>

Published by the [American Institute of Physics](#)

Articles you may be interested in

[Development of a hybrid molecular beam epitaxy deposition system for in situ surface x-ray studies](#)

[Review of Scientific Instruments](#) **89**, 033905 (2018); 10.1063/1.5008369

[Compact low power infrared tube furnace for in situ X-ray powder diffraction](#)

[Review of Scientific Instruments](#) **88**, 013903 (2017); 10.1063/1.4973561

[PDV-based estimation of ejecta particles' mass-velocity function from shock-loaded tin experiment](#)

[Review of Scientific Instruments](#) **89**, 033901 (2018); 10.1063/1.4997365

[Design and performance of an ultra-high vacuum spin-polarized scanning tunneling microscope operating at 30 mK and in a vector magnetic field](#)

[Review of Scientific Instruments](#) **89**, 033902 (2018); 10.1063/1.5020045

[A hydrogen leak-tight, transparent cryogenic sample container for ultracold-neutron transmission measurements](#)

[Review of Scientific Instruments](#) **89**, 033903 (2018); 10.1063/1.4996296

[A fully automated temperature-dependent resistance measurement setup using van der Pauw method](#)

[Review of Scientific Instruments](#) **89**, 033906 (2018); 10.1063/1.4998340

PHYSICS TODAY

WHITEPAPERS

MANAGER'S GUIDE

Accelerate R&D with
Multiphysics Simulation

READ NOW

PRESENTED BY

 COMSOL

Transmission *in situ* and *operando* high temperature X-ray powder diffraction in variable gaseous environments

Lukas Schlicker,^{1,a),b)} Andrew Doran,^{2,b)} Peter Schnepfmüller,¹ Albert Gili,¹ Mathias Czasny,¹ Simon Penner,³ and Aleksander Gurlo¹

¹Fachgebiet Keramische Werkstoffe / Chair of Advanced Ceramic Materials, Institut für Werkstoffwissenschaften- und Technologien, Technische Universität Berlin, Hardenbergstr. 40, D-10623 Berlin, Germany

²Advanced Light Source, Lawrence Berkeley National Laboratory, Berkeley, California 94720, USA

³Institute of Physical Chemistry, University of Innsbruck, Innrain 52c, 6020 Innsbruck, Austria

(Received 25 August 2017; accepted 14 February 2018; published online 6 March 2018)

This work describes a device for time-resolved synchrotron-based *in situ* and *operando* X-ray powder diffraction measurements at elevated temperatures under controllable gaseous environments. The respective gaseous sample environment is realized via a gas-tight capillary-in-capillary design, where the gas flow is achieved through an open-end 0.5 mm capillary located inside a 0.7 mm capillary filled with a sample powder. Thermal mass flow controllers provide appropriate gas flows and computer-controlled on-the-fly gas mixing capabilities. The capillary system is centered inside an infrared heated, proportional integral differential-controlled capillary furnace allowing access to temperatures up to 1000 °C. *Published by AIP Publishing.* <https://doi.org/10.1063/1.5001695>

Time-resolved *in situ* and *operando* X-ray diffraction represents a convenient technique to study changes in crystalline materials induced by heating and/or treatment in defined gaseous environments, as diffraction data provide relatively easy-to-interpret information about the crystalline sample characteristics such as phase composition and (nano)crystallite size and lattice strains. One advantage of the *in situ/operando* X-ray powder diffraction (XRPD) studies conducted at synchrotron sources is the short pattern acquisition time of a few seconds or, depending on the detector and X-ray beam, even less, giving time-resolved insight into transformation kinetics of materials and intermediates of catalytic reactions. In principle, any sample-treatment leading to the formation of new or disappearance of existing crystalline components of the specimen under investigation can be followed in great detail.

Tailored functional materials such as pure or complex oxides or catalytically active nanoparticles supported on various kinds of materials play an ever-increasing role in a wide range of research fields, such as heterogeneous catalysis, gas sensing, or energy conversion. Even the tailor-made materials synthesis process itself is an interesting topic for *in situ* studies.¹ For functional materials, exact knowledge of their structural and physico-chemical behavior under realistic operating conditions significantly adds to the understanding of structure-property correlations. However, the determination of the physico-chemical properties might be restricted by phenomena like phase transformations in simple oxides,² structural alterations such as differing surface/bulk terminations, reconstructions, or in most extreme cases, chemical exsolution effects in complex oxide materials such as spinels and perovskites.³ In catalytic research, different materials

can be tackled by this method. These might also include mono- or intermetallic nanoparticles supported on oxide materials, which are prone to metal-support interaction effects, eventually leading to reactive metal-support interaction and supported intermetallic particles.⁴ In addition, detailed time-resolved investigations of reaction intermediates, e.g., monitoring the formation of deactivating carbon deposits on metal catalysts during methane dry reforming (DRM),⁵ may lead to a better understanding of the underlying reaction mechanisms.

Time-resolved insight into these processes under operating conditions, namely, by *in situ* and *operando* studies, is a key criterion for rational materials and catalyst design and further optimized technical use. Such studies are particularly worthwhile when combined with complementary information from various already well-established characterization methods applicable under exactly the same *in situ* and *operando* conditions: the combination of spectroscopic, electrochemical, physico-chemical, microscopic, and structural studies allows for the establishment of precise and accurate structure-property/activity/selectivity relationships.

The herein described experimental setup, designed and applied at beamline 12.2.2 at the Advanced Light Source (LBNL, California, USA), enables the user to control the most important parameters of realistic operating conditions, namely, temperature, pressure, heating rate, and gaseous atmosphere in a technical environment suitable to conduct *in situ/operando* X-ray diffraction. The authors are aware of the available literature describing numerous comparable approaches specialized for *in situ* studies of, e.g., acid leaching,⁶ 2d-mapping of specimen structures,⁷ or lab-scaled specimen amounts⁸ with some limitations like missing option for capillary rotation or time-consuming glue-based sample preparation.⁹ This note complements the recently published work¹⁰ about an infrared-irradiated SiC tube capillary furnace. This setup, tailor-made for this furnace, is designed to be robust, reliable, and easy to use and with a time-saving sample preparation procedure.

^{a)} Author to whom correspondence should be addressed: schlicker@tu-berlin.de

^{b)} L. Schlicker and A. Doran contributed equally to this work.

software packages. A gas line delivers the mixed gas to the capillary systems (summarized as C, see Fig. 2 for details), to the gas line-in (C-in), and further to a 500 μm injection capillary (E) (capillaries from Hilgenberg GmbH, Germany, depending on experiment temperature available as soda, borosilicate, and quartz glass). The gas leaves the injection capillary at its cut open end at the bottom (bold arrow), where it has intimate contact with the sample powder (F) contained within a 0.7 mm sample capillary (D). The operation of the flow cell is hardly affected by the manufacturing process of the used capillaries in terms of taper shape, funnel length, or quality of the funnel top-edge. The gas flow leaves the system by passing between the walls of D and E (thin arrows) toward the gas line-out (C-out). The line-out is connected to a video-surveyed bubbler (G) to verify gas-tightness at all times during the experiment and finally to an exhaust line (H). In combination with a venting line (J), it allows to purge the gas supply lines after the experiments. As described in Ref. 10, sample heating with defined heating rates and temperatures operates via proportional integral differential (PID)-controlled thermocouples: (e) infrared irradiation [lamps: (a)] of an SiC tube furnace (b) providing entrance slits for the incident X-ray beam (10-30 μm selectable spot size) (c) and diffraction cone (d), which is recorded with suitable detectors (g). The system's centerpiece is represented by part C in Fig. 1: It holds both capillaries D and E and provides gas line-in and line-out via Swagelock quick connectors. The construction consists of three individual parts and two capillaries, as shown in detail in Fig. 2.

For assembly, one proceeds as follows: The gas-injection capillary E with a cut open end is inserted from above into the C2 Teflon fitting, and cap C1 is carefully screwed to C2 until the silicone sealing gets in tight contact with the capillary E funnel edge. Capillary D filled with the sample powder is inserted into the cap C3 Teflon fitting from above; the larger capillary D is pulled over the smaller capillary E by sliding cap C3 and capillary D over E in the bottom to top direction. Finally C3 gets screwed to C2 until C2 silicone sealing and D have close contact. After attaching the quick connects for line-in and line-out, the gas-tightness is tested by applying a gas flow of a few ml/min to C-in. If all connections are tight, gas bubbles should appear in the bubbler G. The complete assembly requires only a few minutes at the beamline, which is a definite advantage of the discussed construction. A clean sample environment can be ensured, as only the replaceable

capillary D is in direct contact to the sample. If sample powders are sensitive to air or humidity, the assembly can even take place inside a glove box under a protective atmosphere. Adjustment of the capillary position with respect to the beam and detector is conducted via the automated DAC centering function at the beamline. At the beginning of each experiment, a LaB₆ NIST standard is measured for detector-to-sample distance and beam calibration. Improved powder statistics, e.g., in the case of coarse-crystalline samples, is achieved by oscillating the capillary and tube furnace together by moving the beamline sample stand equipped with high-precision stepper motors in a X-Y-plane perpendicular to the beam within the limits allowed by the 800 μm diameter furnace beam entrance hole. Superposition of two oscillations in the X and Y directions (Z is the direction of the beam) with purposefully selected different frequencies and lengths cover enough sample volume for improved powder statistics. The impact of the described sample movement is illustrated in the following Fig. 3: two detector images were recorded with and without sample oscillation. The detector image recorded while oscillating the sample (a) shows almost complete rings for all reflexes and therefore improved powder statistics. Compared to that, a fixed sample results in the spotty detector image shown in (b).

Test measurements (Fig. 4) across the whole sample powder column inside the capillary have shown that the entire sample reacts homogeneously with the gas, and accordingly, no differences in the patterns arise. To confirm a complete reaction across the entire capillary, a test measurement was conducted in the following configuration: A 0.7 mm sample capillary was filled with a 3 mm powder column at its bottom-end. The sample powder consisted of oxide supported on nanocrystalline mixed *t*- and *m*-ZrO₂.

In a first run, the sample was oxidized by heating from 30 °C to 400 °C at 20 °C/min heating rate under 4 ml/min O₂ flow. After cooling to room temperature, the tube furnace was removed to take three patterns from the bottom (B), middle (M), and top (T) regions of the 3 mm sample column, as denoted in the schematic representation in Fig. 4. In a second run, the sample was subjected to the reduction treatment by heating from 30 °C to 300 °C at 20 °C/min heating rate under 4 ml/min H₂ flow. Subsequently three patterns at B, M, and T sites were taken. The recorded patterns are shown in the right panel of the graph in Fig. 4 and clearly indicate that oxidation as well as reduction took place evenly and reproducibly across

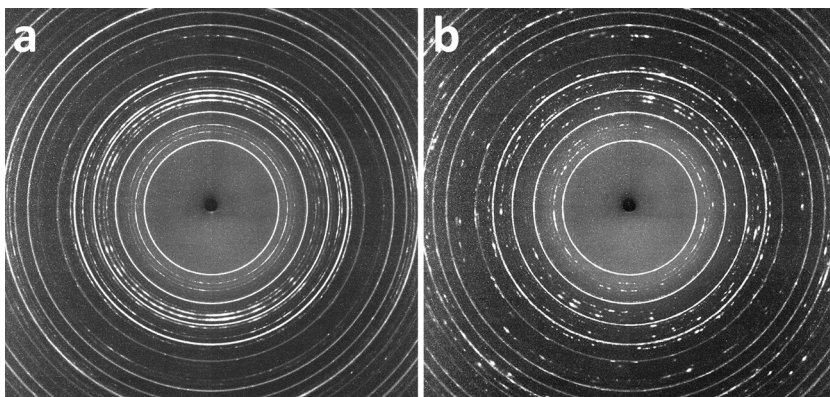


FIG. 3. Representative patterns with (a) and without (b) in-plane movement of a Li₂SiO₃ + Li₂CO₃ containing sample from the CO₂ absorption application example shown below.

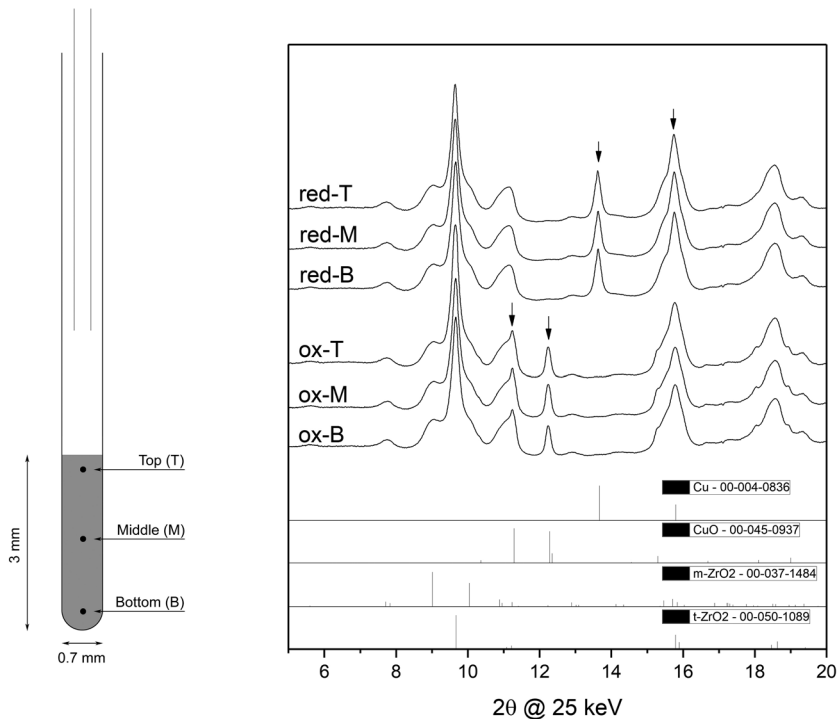


FIG. 4. Schematic sketch of the test measurement configuration and resulting patterns recorded after oxidation and reduction at bottom (B), middle (M), and top (T) parts of the sample powder column.

the entire sample, with no significant difference in the patterns measured across the sample.

As for gas-leaking, this system so far was used numerous times for experiments with various gases including pure oxygen and hydrogen or methane-containing gas mixtures at elevated temperatures up to 1000 °C without any leaking events. If the bottom capillary tip is free-standing and not touching the tube wall or the thermocouple residing 2-3 mm below the tube tip, the capillary withstands the conditions during the experiment without breaking. This safety issue is further addressed by continuous observation of the video surveyed bubbler (G in Fig. 1) during the experiment which helps us to monitor interruptions of the outgoing gas flow as indication of a leaking event. However, additional gas flow meters

at C-in and C-out will be installed to compare incoming and outgoing flows with automatic shut-down of gas supply and heating in the case of $\text{flow}_{\text{C-out}} < \text{flow}_{\text{C-in}}$.

Extension of the experimental setup, e.g., via connection of a mass spectrometer, at the C-out side for studying the composition of the gas mixture at the end of the heated capillary system to eventually combine structural transformations of the sample with changes in the gas composition is envisioned and possible.

The carbon dioxide absorption in Li_4SiO_2 as described in Ref. 11 serves as an illuminating application example, highlighting the capabilities of the setup: Li_4SiO_2 was heated to 700 °C, held isothermally for 2 min, and re-cooled back to room temperature in CO_2 flow while one pattern per 30 s was recorded.

Figure 5 shows how the initial Li_4SiO_2 related reflections disappear upon reaching the final temperature while new reflections of Li_2SiO_3 appear. Upon cooling back down, a second appearing set of reflections can be assigned to Li_2CO_3 . The whole process follows the mechanism for carbon dioxide chemisorption as described by $\text{Li}_4\text{SiO}_2 + \text{CO}_2 \rightarrow \text{Li}_2\text{SiO}_3 + \text{Li}_2\text{CO}_3$.

Further studies conducted with this setup can be found in Refs. 2, 12, and 13: the dependence of the t-ZrO₂ phase transformation on the gaseous environment,¹² stability of rh-In₂O₃ in different gases,² and iron-exsolution phenomena in $\text{La}_{0.6}\text{Sr}_{0.4}\text{FeO}_{3-d}$ under reductive conditions¹³ have been studied.

See [supplementary material](#) for four figures with technical drawings of assembled part C as well as the single pieces C1, C2, and C3.

This work conducted within AP Program No. ALS-08865 used resources of the Advanced Light Source, which is a DOE

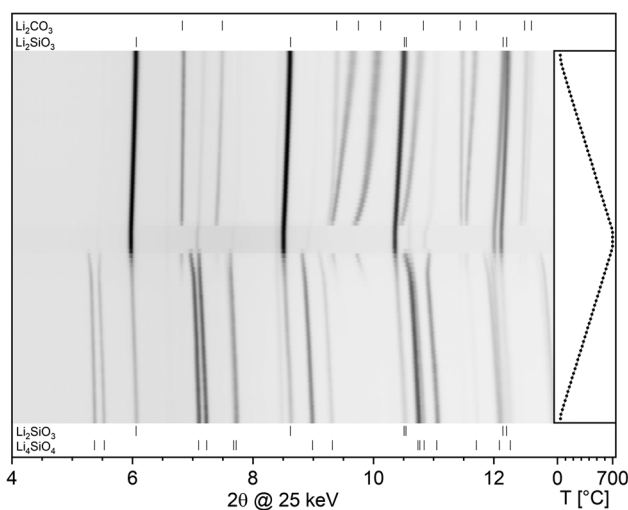


FIG. 5. XRPD phase evolution of Li_4SiO_3 treated in CO_2 .

Office of Science User Facility under Contract No. DE-AC02-05CH11231. L.S. appreciates the funding of his research with an ALS doctoral fellowship. This work is part of the Cluster of Excellence “Unifying Concepts in Catalysis” coordinated by the Technische Universität Berlin. Financial support by the Deutsche Forschungsgemeinschaft (DFG) within the framework of the German Initiative for Excellence is gratefully acknowledged. Part of the work was conducted within the framework of the special research platform “Materials and Nanoscience” at the University of Innsbruck.

¹T. M. Mattox, C. Groome, A. Doran, C. M. Beavers, and J. J. Urban, *Solid State Commun.* **265**, 47 (2017).

²E. M. Kock, M. Kogler, C. Zhuo, L. Schlicker, M. F. Bekheet, A. Doran, A. Gurlo, and S. Penner, *Phys. Chem. Chem. Phys.* **19**, 19407 (2017).

³R. Thalinger, M. Gocyla, M. Heggen, B. Klotzer, and S. Penner, *J. Phys. Chem. C* **119**, 22050 (2015).

⁴S. Penner and M. Armbruster, *ChemCatChem* **7**, 534 (2015).

⁵P. W. Menezes, A. Indra, P. Littlewood, C. Gobel, R. Schomacker, and M. Driess, *ChemPlusChem* **81**, 370 (2016).

⁶I. C. Madsen, N. V. Y. Scarlett, and B. I. Whittington, *J. Appl. Crystallogr.* **38**, 927 (2005).

⁷J. D. Grunwaldt, S. Hannemann, C. G. Schroer, and A. Baiker, *J. Phys. Chem. B* **110**, 8674 (2006).

⁸S. J. Moorhouse, N. Vranješ, A. Jupe, M. Drakopoulos, and D. O’Hare, *Rev. Sci. Instrum.* **83**, 084101 (2012).

⁹T. R. Jensen, T. K. Nielsen, Y. Filinchuk, J. E. Jorgensen, Y. Cerenius, E. M. Gray, and C. J. Webb, *J. Appl. Crystallogr.* **43**, 1456 (2010).

¹⁰A. Doran, L. Schlicker, C. M. Beavers, S. Bhat, M. F. Bekheet, and A. Gurlo, *Rev. Sci. Instrum.* **88**, 013903 (2017).

¹¹K. Yamauchi, N. Murayama, and J. Shibata, *Mater. Trans.* **48**, 2739 (2007).

¹²E. M. Kock, M. Kogler, T. Gotsch, L. Schlicker, M. F. Bekheet, A. Doran, A. Gurlo, B. Klotzer, B. Petermuller, D. Schildhammer, N. Yigit, and S. Penner, *Dalton Trans.* **46**, 4554 (2017).

¹³T. Götsch, C. Praty, M. Grünbacher, L. Schlicker, M. F. Bekheet, A. Doran, A. Gurlo, M. Tada, H. Matsui, N. Ishiguro, B. Klotzer, and S. Penner, *ECS Trans.* **78**, 1327 (2017).